Dynamic Mechanical Interactions Between Neighboring Airspaces Determine Cyclic Opening and Closure in Injured Lung

Ludovic Broche, PhD[1,2]; Gaetano Perchiazzi, MD, PhD[3,4]; Liisa Porra, PhD[5,6]; Angela Tannoia, MD[4]; Mariangela Pellegrini, MD[3,4]; Savino Derosa, MD[4]; Alessandra Sindaco, MD[4]; João Batista Borges, MD, PhD[3,7]; Loïc Degrugilliers, MSc[2]; Anders Larsson, MD, PhD[3]; Göran Hedenstierna, MD, PhD[8]; Anthony S. Wexler, PhD[9]; Alberto Bravin, PhD[1]; Sylvia Verbanck, PhD[10]; Bradford J. Smith, PhD[11]; Jason H. T. Bates, PhD[11]; Sam Bayat, MD, PhD[2]

[1]European Synchrotron Radiation Facility, ID17 Biomedical Beamline, Grenoble, France.

[2]Department of Pediatric Pulmonology, Université de Picardie Jules Verne, Inserm U1105 & Amiens University Hospital, Amiens, France.

[3]Hedenstierna Laboratory, Department of Surgical Sciences, Section of Anaesthesiology & Critical Care, Uppsala University, Uppsala, Sweden.

[4]Department of Emergency and Organ Transplant, University of Bari, Bari, Italy.

[5]Department of Physics, University of Helsinki, Helsinki, Finland.

[6]Helsinki University Central Hospital, Helsinki, Finland.

[7]Pulmonary Division, Cardio-Pulmonary Department, Heart Institute (Incor), University of São Paulo, São Paulo, Brazil.

[8]Hedenstierna Laboratory, Department of Medical Sciences, Clinical Physiology, Uppsala University, Uppsala, Sweden.

[9]Department of Mechanical Engineering and Environmental Quality Laboratory, University of California Davis, Davis, CA.

[10]Respiratory Division, University Hospital UZ Brussel, Brussels, Belgium.

[11]Department of Medicine, University of Vermont, Burlington, VT.

Work performed at the European Synchrotron Radiation Facility.

Supplemental digital content is available for this article. Direct URL citations appear in the printed text and are provided in the HTML and PDF versions of this article on the journal's website (http://journals.lww.com/ccmjournal).

Supported, in part, by the Swedish Heart, the Lung foundation and the Swedish Research Council (K2015-99X-22731-01-4); the Picardie Regional Council; the European Synchrotron Radiation Facility; the Bari University; the Tampere Tuberculosis Foundation Finland; and the United States National Institutes of Health (1 R01 HL124052 and 1 K99 HL128944).

Dr. Broche received support for article research from the Picardie Regional Council and the European Synchrotron Radiation Facility. Dr. Porra received support received support for article research from the Tampere Tuberculosis Foundation Finland. Dr. Perchiazzi received support for article research from the Bari University. Dr. Larsson received support for article research from the Swedish Research Council (Vetenskapsrådet-VR). His institution received funding from the Swedish Research Council and from the Swedish Heart and Lung Foundation. Dr. Smith received support for article research from the National Institutes of Health (NIH). Dr. Bates received support for article research from the NIH. His institution received funding from the NIH-National Heart, Lung and Blood Institute. Dr. Bayat received funding from Novartis pharmaceuticals (one-time fee for lecture). The remaining authors have disclosed that they do not have any potential conflicts of interest.

For information regarding this article, E-mail: broche@esrf.fr; broche.ludovic@gmail.com

DOI: 10.1097/CCM.0000000000002234

Objectives: Positive pressure ventilation exposes the lung to mechanical stresses that can exacerbate injury. The exact mechanism of this pathologic process remains elusive. The goal of this study was to describe recruitment/derecruitment at acinar length scales over short-time frames and test the hypothesis that mechanical interdependence between neighboring lung units determines the spatial and temporal distributions of recruitment/derecruitment, using a computational model.

Design: Experimental animal study.

Setting: International synchrotron radiation laboratory.

Subjects: Four anesthetized rabbits, ventilated in pressure controlled mode.

Interventions: The lung was consecutively imaged at ~ 1.5-minute intervals using phase-contrast synchrotron imaging, at positive end-expiratory pressures of 12, 9, 6, 3, and 0 cm H_2O before and after lavage and mechanical ventilation induced injury. The extent and spatial distribution of recruitment/derecruitment was analyzed by subtracting subsequent images. In a realistic lung structure, we implemented a mechanistic model in which each unit has individual pressures and speeds of opening and closing. Derecruited and recruited lung fractions ($F_{derecruited}$, $F_{recruited}$) were computed based on the comparison of the aerated volumes at successive time points.

Measurements and Main Results: Alternative recruitment/derecruitment occurred in neighboring alveoli over short-time scales in all tested positive end-expiratory pressure levels and despite stable pressure controlled mode. The computational model reproduced this behavior only when parenchymal interdependence

between neighboring acini was accounted for. Simulations closely mimicked the experimental magnitude of $F_{derecruited}$ and $F_{recruited}$ when mechanical interdependence was included, while its exclusion gave $F_{recruited}$ values of zero at positive end-expiratory pressure greater than or equal to 3 cm H_2O.

Conclusions: These findings give further insight into the microscopic behavior of the injured lung and provide a means of testing protective-ventilation strategies to prevent recruitment/derecruitment and subsequent lung damage. (*Crit Care Med* 2016; XX:00–00)

Key Words: acute respiratory distress syndrome; assisted ventilation; imaging/computed tomography; pulmonary oedema; synchrotron

Patients with acute respiratory distress syndrome (ARDS) invariably require mechanical ventilation in order to manage the work of breathing and improve gas exchange. Despite the indisputable effectiveness of this therapy, positive pressure ventilation imposes mechanical stresses on the parenchyma that can worsen lung injury, a condition known as "ventilator-induced lung injury" (VILI) (1–3).

The exact mechanisms leading to VILI at the acinar level remain elusive, although it is generally accepted that mechanical strain due to exaggerated deformation at the cellular level can lead both to structural deterioration and inflammation of the parenchyma through mechanotransduction responses (4, 5). In particular, high pressure and large volume excursions have been demonstrated to induce mechanical injury in the lung (1). This mechanism, termed "volutrauma," is suggested by the decrease in mortality in ARDS patients observed when tidal volume (VT) and plateau pressures are limited (6, 7). Nevertheless, low VT can still lead to injury (2, 8) by potentiating inflammation through three mechanisms that are unrelated to volutrauma, namely: 1) cyclic recruitment/derecruitment (R/D) of peripheral airspaces, referred to "atelectrauma" (9); 2) displacement of air-liquid interfaces along small airways, which injures epithelial cells (10, 11); and 3) mechanical interdependence, which causes the pulling forces between adjacent aerated and collapsed alveoli to produce local pressures that substantially surpass transpulmonary pressure (12–14).

The R/D events giving rise to VILI are dynamic, occurring more or less rapidly depending on the severity of lung injury (14, 15), whether recruitment maneuvers have been applied, and what mechanical ventilation settings, such as positive end-expiratory pressure (PEEP) and driving pressure, are employed (16). Previously, Ma and Bates (17) proposed a computational model of R/D dynamics based on a symmetrically bifurcating airway tree in which each branch has a critical closing and opening pressure as well as opening and closing speeds. This model has successfully reproduced the observed time-dependent changes in lung elastance observed the following deep inspiration maneuvers in experimental models of VILI in mice (18), suggesting that it captures essential aspects of R/D dynamics.

However, this model makes no predictions about how VILI is distributed throughout the lung, while the lung damage that occurs in VILI is known to be spatially heterogeneous. Furthermore, the presence of mechanical interdependence between adjacent regions of the lung parenchyma suggests that VILI, and the R/D events that cause it, is likely to be spatially correlated (13, 18). In addition, the dynamic nature of R/D suggests that the extent and distribution of VILI is highly dependent on pressure and volume history (17), and that the R/D that occurs over short-time scales (order of minutes [19]) has a strong influence on lung aeration and mechanics over longer periods of time (order of hours). The pathogenesis of VILI is thus likely to be critically determined by the short-term temporal dynamics of R/D and their spatial distribution at the acinar level, yet we currently have little understanding of either phenomenon.

Accordingly, the present study was undertaken to quantify the extent and distribution of R/D at the acinar scale in a lavage-induced rabbit model of VILI using in vivo synchrotron radiation phase-contrast imaging. Using a computational model based on that of Ma and Bates (17) adapted to include a morphologically realistic 3D airway tree, we investigated the hypothesis that mechanical interaction between neighboring terminal lung units could potentially contribute to our experimental observations.

METHODS

A detailed description of the experimental procedures is provided in the **supplementary materials** (Supplemental Digital Content 1, http://links.lww.com/CCM/C290). The care of animals and the experimental procedures were in accordance with the Directive 2010/63/EU of the European Parliament and were approved by the Evaluation Committee for Animal Welfare of the European Synchrotron Radiation Facility. Briefly, the experiments were performed on four male New Zealand rabbits. The animals were anesthetized, paralyzed, and mechanically ventilated in pressure controlled mode (PCV) mode, with a pressure above PEEP set in order to obtain a VT of 6 mL/kg; F_{IO_2} of 0.6; I:E ratio of 1:2; a baseline PEEP of 3 cm H_2O; and a respiratory rate set to obtain a Pa_{CO_2} of approximately 40 mm Hg. Plateau pressure was limited to 35 cm H_2O. Animals were immobilized in the upright position for imaging. We used synchrotron phase-contrast CT imaging (20, 21) with an acquisition time of 21.7 seconds for a 2.5 mm thick volume at a voxel size of 47.5 μm^3.

Study Protocol

The imaging protocol started with a recruitment maneuver (20 cm H_2O, 10 s). The lung was imaged nine times at end-expiration at approximately 1.5-minute intervals at each subsequent PEEP level of 12, 9, 6, 3, and 0 cm H_2O. Thereafter, the rabbits underwent five sequential whole lung normal saline lavages (100 mL/kg), followed by 120 minutes of injurious ventilation with a peak inspiratory pressure of 35 cm H_2O, zero PEEP, respiratory rate of 20/min, and F_{IO_2} of 100%. Following injurious ventilation, the same imaging protocol was repeated.

Simulation of R/D in a Realistic Airway Tree Structure

In a morphologically realistic right rabbit lung airway tree (**Fig. 4*A***), we implemented a computational model in which each

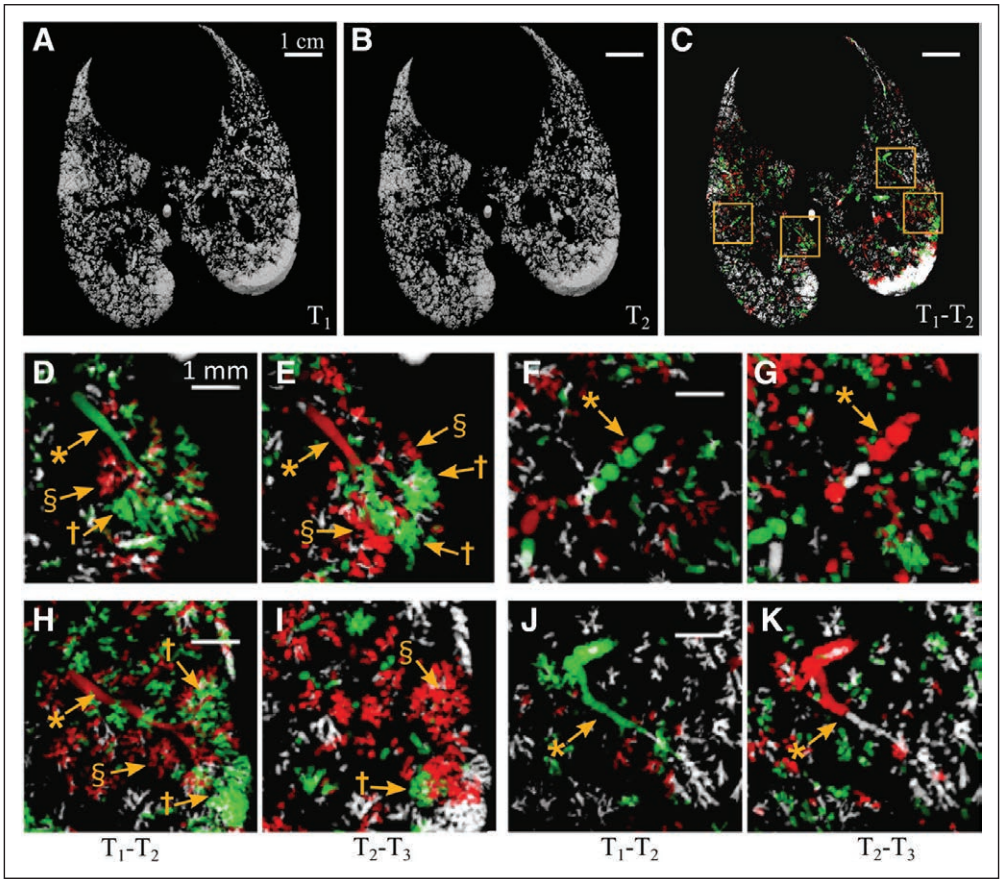

Figure 1. Alveolar recruitment/derecruitment (R/D) occurring alternately in neighboring lung units over short-time scales ~ 1 min, in injured lung at positive end-expiratory pressure (PEEP) 6 cm H_2O. **A**–**C**, 3D renderings of aerated lung regions obtained by segmentation of synchrotron phase-contrast CT images at 0 (**A**) and 84 s (**B**) in a 2.5 mm thick slice, in injured lung at PEEP 6 cm H_2O; **C**, R/D map quantified using image registration between T_1 (**A**) and T_2 (**B**). *White*: aerated, no change; *black*: nonaerated, no change; *green*: opening; and *red*: closing. *Yellow squares* delineate regions of interest magnified in **D**–**K** with **D**, **F**, **H**, and **J** computed from two successive images acquired at 0 and 84 s (T_2–T_1) and **E**, **G**, **I**, and **K** from the subsequent time interval between 84 and 159 s (T_3–T_2). *bronchioles, †recruiting airspaces, and §derecruiting airspaces. Raw images are shown in Figure S3 (Supplemental Digital Content 1, http://links.lww.com/CCM/C292).

airway and acinar unit has an opening and closing pressure as well as an opening and closing speed according to Bates and Irvin (15). The model was modified to account for the PCV mode of ventilation and to include mechanical interdependence between neighboring acini; at each time point, the opening and closing pressures of a given unit depended on the state of each surrounding unit in inverse proportion to the square of their separation distance and in direct proportion to their relative volumes.

RESULTS

Lung injury was severe with a significant decrease in the Pao_2/Fio_2 ratio (528 ± 52 to 115 ± 47 mm Hg) and in respiratory compliance (2.78 ± 0.14 to 0.22 ± 0.09 mL/cm H_2O; **Table S2**, Supplemental Digital Content 2, http://links.lww.com/CCM/C291).

Figure 1, *A* and *B* shows volumetric renderings of the aerated fraction obtained by segmentation of two images acquired 84 seconds apart in a representative injured lung at PEEP 6 cm H_2O. Corresponding raw CT slices are shown in **Figure S3** (Supplemental Digital Content 1, http://links.lww.com/CCM/C292). Figure 1***C*** shows a volumetric map of the changes in regional lung aeration from one time point to the next, computed using registration of the sequential images. Four regions of interest within the parenchyma are enlarged in Figure 1, ***D*–*K***. Figure 1, *D*, *F*, *H*, and *J* shows the differences in aeration between time T_1 and T_2, whereas Figure 1, *E*, *I*, *G*, and *K* shows those between T_2 and T_3. First, these images show that the postinjury regional distribution of lung aeration was spatially heterogeneous. Second, we identified both aerated (white) and nonaerated (black) lung regions that were stable over the imaged time intervals, as well as other regions that were highly unstable over the same time course. A remarkable finding was that adjacent and communicating airspaces subtended by the same terminal airway did not all behave in the same way, but rather exhibited alternating patterns of recruitment and derecruitment. Indeed, in Figure 1*D*, a terminal airway (*) and part of an acinus (†) are recruited, whereas other regions within the acinus are either closing (§) or remain closed. Thirty respiratory cycles later (Fig. 1*E*) the terminal airway has closed (*), and some regions of the subtended acinus are opening (†) while closely adjacent areas to these are closing (§). Figure 1, *H* and *I* shows an example of the closure of a small airway (*), which remained closed in the following time interval, while subtended acinar regions were closing (§) and opening (†). Similar findings were obtained in the other animals and are included in **Figure S4** (Supplemental Digital Content 3, http://links.lww.com/CCM/C293). On rare occasions (Fig. 1, *F* and *G*), the images suggest the presence of liquid bridges moving within the airway lumen (*). However, in the majority of cases, complete small airway closure occurred along a certain airway length (Fig. 1, *J* and *K*).

Interestingly, R/D occurred in the face of perfectly stable mechanical ventilation settings and in spite of the fact that the animals were ventilated in PCV mode. In all animals, unequal magnitude of recruitment and derecruitment led to fluctuations in the aerated lung fraction at each PEEP level, as illustrated in **Figure 2**. Initially, the average aeration in the imaged lung differed between animals, likely due to disparity in the

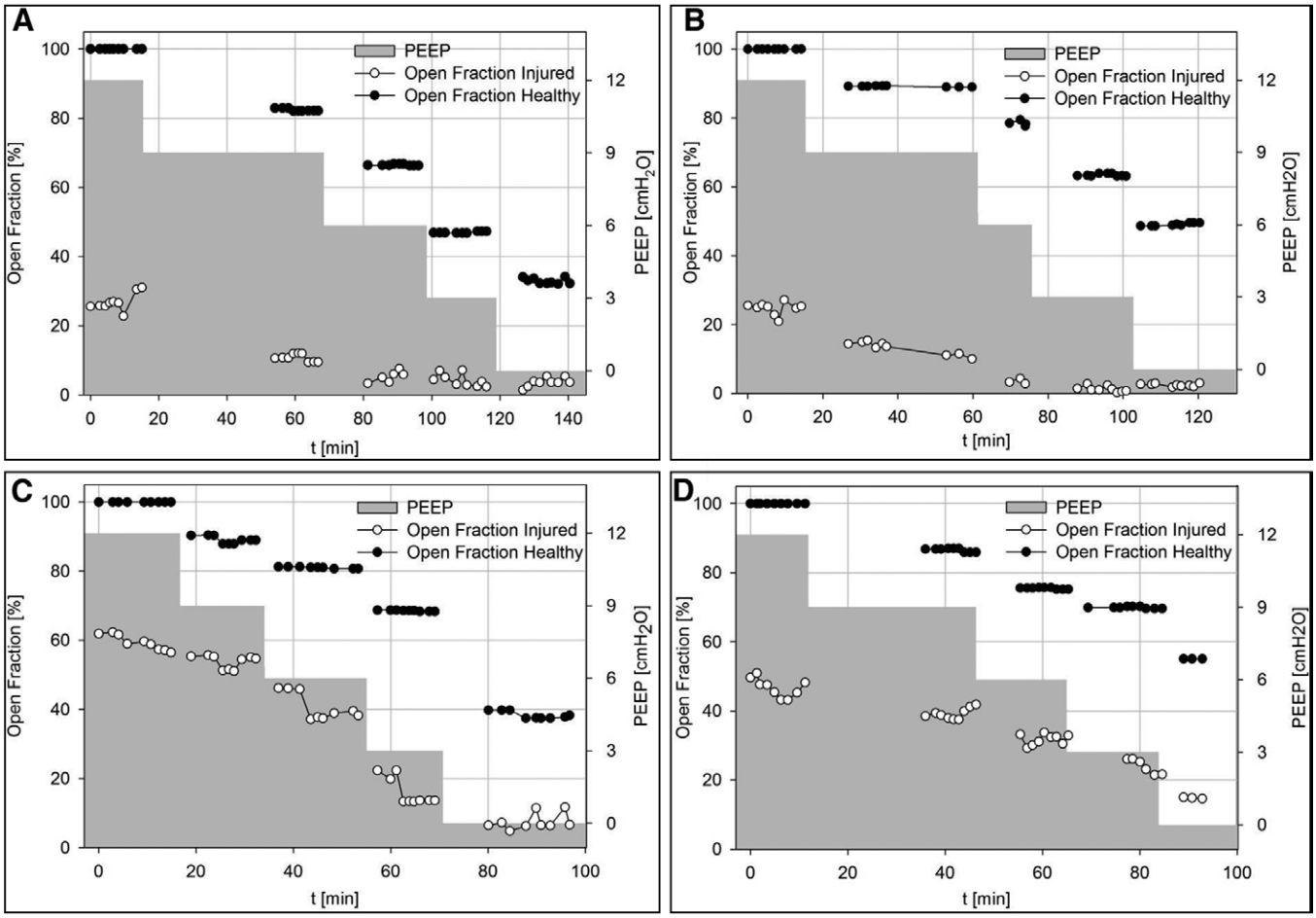

Figure 2. Short-term history of aerated lung fraction versus time and positive end-expiratory pressure (PEEP) level: experimental data at baseline and after lung injury. Aerated fraction expressed as percentage of baseline lung volume at PEEP 12 cm H_2O. *Black*: healthy lung, *white*: injured lung, and *grey*: PEEP history. **A–D**, experimental data in rabbits 1–4, respectively.

severity of lung injury. Although the average aeration of the injured lung improved with PEEP, the short-term fluctuations in aeration fraction were observed at all PEEP levels including the highest level of 12 cm H_2O.

Figure 3, ***A*** and ***D*** shows the fractions of derecruited and recruited lung volume ($F_{recruited}$, $F_{derecruited}$; see **supplemental Methods**, Supplemental Digital Content 1, http://links.lww.com/CCM/C290) calculated between two consecutive scans. The magnitude of R and D was not different for PEEP levels greater than or equal to 6 cm H_2O. However, $F_{derecruited}$ significantly increased below this PEEP level, whereas the increase in $F_{recruited}$ was not statistically significant.

The cardinal features of the experimental findings were reproduced in silico, by the model proposed by Ma (17) modified to include mechanical interdependence between acinar parenchyma. In the simulation of a normal lung (**Fig. 4**, ***A*** and ***B***, black symbols), the model produced no fluctuations of the aerated fraction at the end of expiration. In the simulation of an injured lung (Fig. 5*A*, white symbols), the model mimicked the experimental fluctuations in aerated fraction over short-time intervals despite PCV (compare with experimental data in Fig. 2). An illustration of such fluctuations under PEEP 6 cm H_2O is presented in **Figure 5*B***. These instabilities were due to successive R/D as illustrated in **Figure 5**, ***C*** and ***D*** where it can be appreciated that the distribution of R/D was spatially correlated, that is, adjacent units alternately recruited and derecruited over the same short-time interval. Furthermore, the model yielded to $F_{recruited}$ and $F_{derecruited}$ values that were similar in magnitude and in dependence upon PEEP, to the experimental values (Fig. 3, ***B*** and ***E***).

When the mechanical interdependence was not included in the computational model, both the temporal volume fluctuations and the spatial R/D correlation disappeared (Fig. 5*B*). In this case, the fractional aeration merely showed a decrease as a result of progressive derecruitment with time. Short-term dynamics and spatial distributions of R/D in the computational model are exemplified in **Video S1** (Supplemental Digital Content 5, http://links.lww.com/CCM/C321). Under this condition, the $F_{derecruited}$ values rose more rapidly with decreasing PEEP than in the case where peripheral lung units were mechanically interdependent (Fig. 3, ***C*** and ***F***). Conversely, $F_{recruited}$ was zero above PEEP 3 and increased only below this PEEP level.

DISCUSSION

In this study, the comparison of serial volumetric phase-contrast synchrotron images of the injured lung revealed dynamic regional R/D of terminal airways and acini over short-time

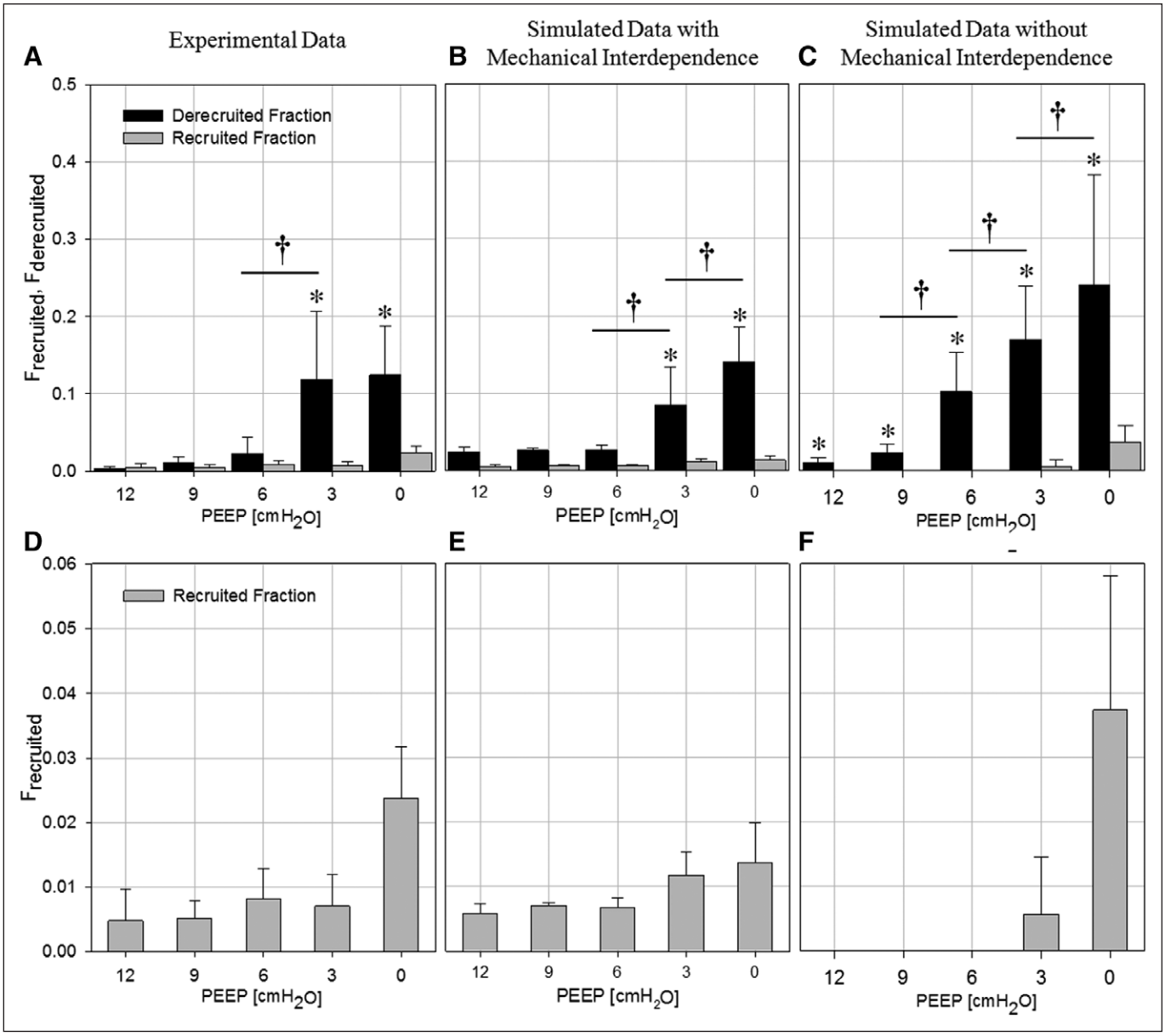

Figure 3. Fractions of recruited ($F_{recruited}$) and derecruited ($F_{derecruited}$) lung. Data are mean ± SD for all animals and time intervals, or time intervals only for simulations. **A** and **D**, experimental data; **B** and **E**, simulated data including mechanical interdependence between peripheral lung units; **C** and **F**, simulated data not including mechanical interdependence; **D**–**F**, enlarged scale for $F_{recruited}$. †$p < 0.001$ versus positive end-expiratory pressure (PEEP) level; *$p < 0.001$ versus $F_{derecruited}$.

intervals on the order of 1.5 minutes. We found that adjacent and communicating airspaces subtended by the same terminal airway did not all behave in the same way, but rather exhibited alternating patterns of recruitment and derecruitment implying that they are influencing each other's behavior. These patterns of R/D occurred in spite of mechanical ventilation being under pressure control with constant settings. The short-term fluctuations in aeration fraction as a result of unbalanced R/D were observed at all PEEP levels, even at the highest PEEP of 12 cm H_2O. To our knowledge, this is the first experimental observation of such phenomena at this spatial resolution in the lung in situ.

Previous theoretical studies of VILI have suggested that the expansion of aerated alveoli in the vicinity of collapsed alveoli produces stress concentrations in the lung tissue close to the interface between these regions (12–14). Exaggerated mechanical stress is thought to potentially trigger or amplify inflammation, which could worsen lung injury (4, 9). The experimental demonstration that R/D phenomena occurred at small length scales and within the same time intervals in adjacent regions of the lung is therefore highly significant. Closer examination of our images (Fig. 1, *D–K*) suggests that the total closure of small peripheral airways occurred over a limited length along the airways and resulted in gas trapping in the subtended acinar region.

It has been suggested that small airways can close due to fluid-elastic instabilities that lead to the formation of liquid

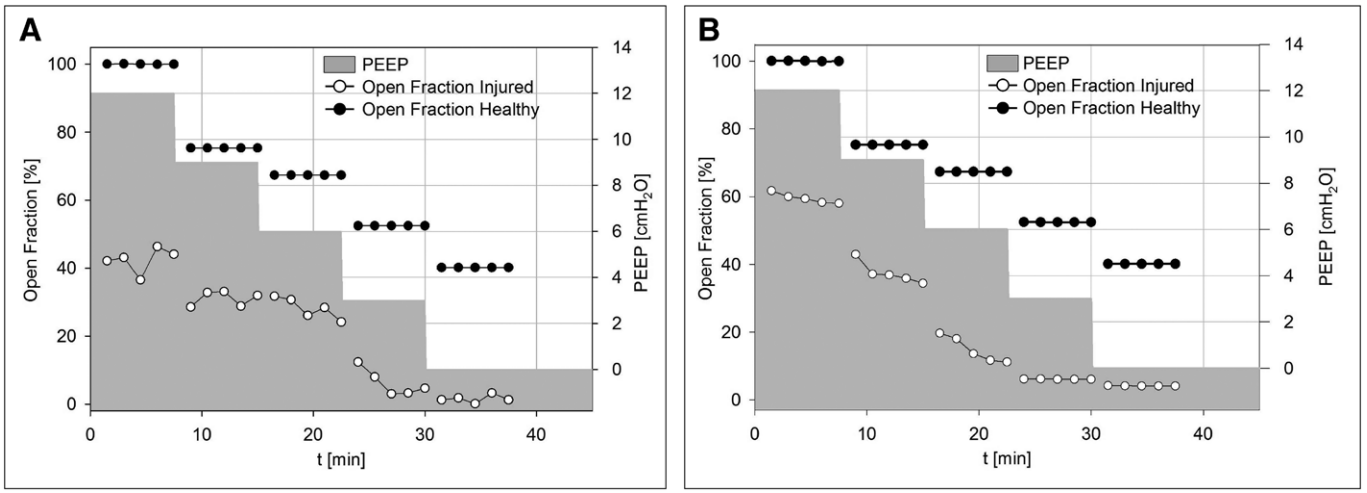

Figure 4. Short-term history of aerated lung fraction versus time and positive end-expiratory pressure (PEEP) level: in simulated data. Aerated fraction expressed as percentage of baseline lung volume at PEEP 12 cm H_2O. *Black*: healthy lung, *white*: injured lung, and *gray*: PEEP time course. **A**, simulated data including mechanical interdependence between airway units; **B**, simulated data without mechanical interdependence between airway units.

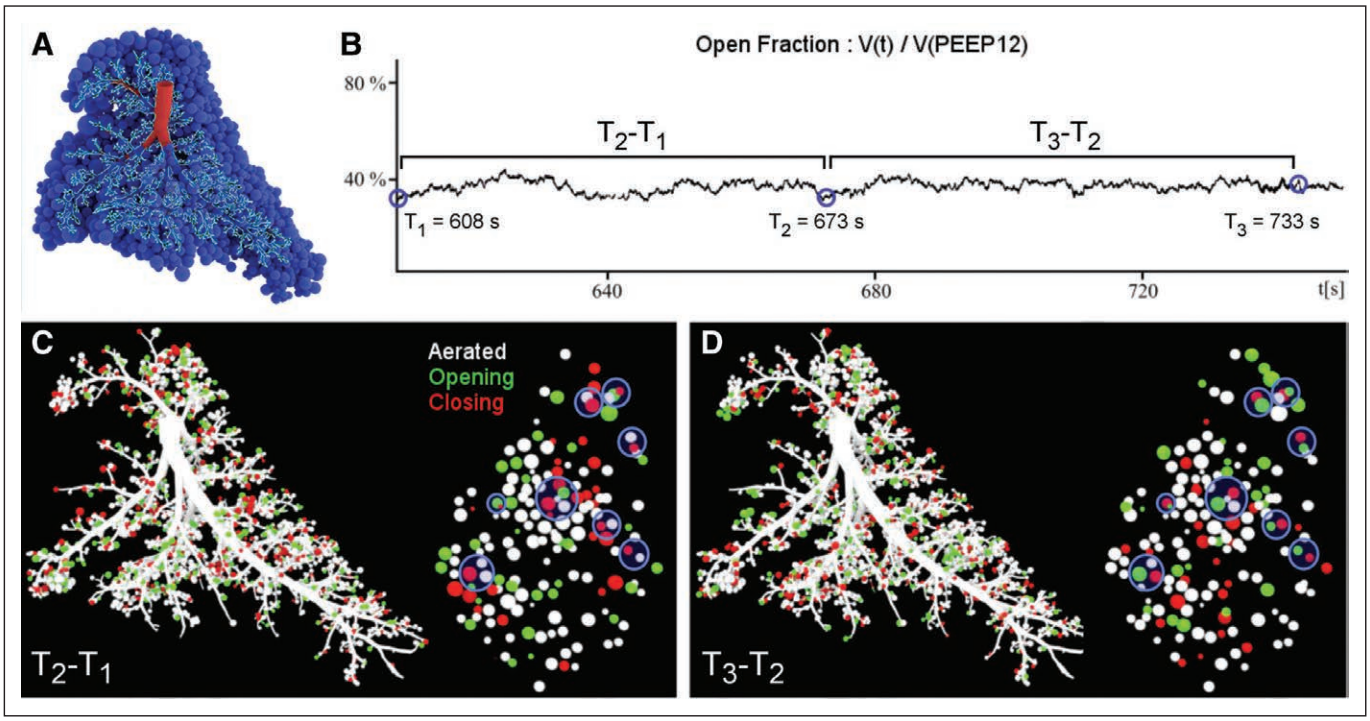

Figure 5. Computational simulation of airway and acinar behavior under positive pressure ventilation in injured lung, in a 3D morphologically realistic right rabbit lung at positive end-expiratory pressure (PEEP) 6 cm H_2O. **A**, right lung structural model comprising 7,175 airways feeding 3,843 acinar units. **B**, short-term changes of the lung open fraction over time; three arbitrary time points approximately 1 min apart are selected for comparison with the experimental data. **C** and **D**, recruitment/derecruitment (R/D) distribution computed in between the three selected time points. *White*: stable aerated; *black*: stable collapsed; *green*: opening (recruitment); *red*: closing (derecruitment); and *blue circles*: alternating R/D behavior. Distributions are shown for the same time points as in **B**. *Left*: Full lung; *right*: 2 mm slice similar to the experimental images.

bridges and subsequent collapse of the airway wall (22). This mechanism, termed "compliant collapse," is more likely to occur when the surface tension of the airway lining liquid is increased, as was the case due to the lung injury induced in the present study, and in small peripheral airways with more compliant walls (22, 23). An alternative mechanism that has been proposed is liquid occlusion due to the formation of menisci (24). This mechanism is promoted by the excess of airway lining liquid which was also likely the case in the present study. Indeed, on a few occasions, we observed liquid menisci within the airways, manifest as dense bridges across the airway lumen (Fig. 1, *C* and *G*). Although the latter mechanism cannot be excluded, our experimental data suggest that compliant collapse probably was the predominant cause of airway closure.

We also observed the curious phenomenon of collapsed lung regions becoming recruited at end-expiratory pressure,

in a few breathing cycles and in PCV mode, which is not predicted by the original computational model of Ma and Bates (17). In that model, R/D phenomena are time dependent as a result of airway opening and closure speeds that reflect the dynamics of formation and disruption of liquid bridges. In the model, since PC implies that the intraluminal pressure varies between the PEEP level and a set maximal pressure during inspiration, a nonaerated unit at the end of expiration will be closed in expiration through all forthcoming breathing cycles. This does not, however, take into account the possible effects of mechanical interdependence (12, 25). We therefore modified the model by considering a morphologically realistic airway tree where the linear distance between any given pair of lung units was known. By modeling the effects of mechanical interdependence between neighboring acini, we simulated how closure of a unit affects the critical opening and closing pressures of nearby units, thereby mimicking the change in stress distribution within the parenchymal network (13). Furthermore, the comparison of $F_{\text{derecruited}}$ and $F_{\text{recruited}}$ between the experimental data and model simulation showed a close agreement only when mechanical interdependence between peripheral lung units was simulated (Fig. 3*B*). The simulated outputs show that when mechanical interdependence is included, alternating R/D of neighboring units can indeed occur despite stable PCV settings, whereas this phenomenon was far more limited in the opposite case, resulting merely in a pendelluft effect within trapped lung regions below PEEP 6 cm H_2O (Video S1, Supplemental Digital Content 5, http://links.lww.com/CCM/C321). Also, the more rapid derecruitment in the absence of mechanical interaction can be attributed to the stabilizing effect of the mutual structural support provided by the interconnected acinar structures. These findings suggest that the dynamic nature of opening and closing and the mechanical interdependence between adjacent peripheral lung units are sufficient conditions for R/D to occur in alternating patterns during PCV.

Another important finding in this study is that although R/D phenomena were reduced by increasing PEEP, they were still present even at the highest PEEP of 12 cm H_2O. We assume that the severity of injury did not significantly evolve during the course of postinjury data acquisition (~ 2 hr), based on pilot studies. An interpretation of this finding is that the critical opening and closing pressures are scattered over a wide range of values (26). This means that a significant proportion of the airspaces have opening and closing pressures that remain within the driving pressure range, making them vulnerable to cyclic R/D.

These findings may have translational implications in terms of detecting R/D in a clinical setting. Indeed, we noticed that R/D caused sudden small-amplitude spikes in the flow curve monitored at the airway opening. Previously, Hantos et al (27) used transients in the airway flow signal from isolated dog lung lobes to detect reopening of collapsed lung regions via avalanches, analogous to those observed in our imaging data. Similarly, Victorino et al (28) showed sudden lung volume increases when collapsed lung was reopened during a sustained insufflation. We speculate that these flow signals could be used to monitor R/D phenomena continuously in patients with ARDS and hence personalize mechanical ventilation settings aiming at minimizing R/D.

CONCLUSIONS

In summary, synchrotron phase-contrast imaging allowed us to visualize dynamic regional R/D of terminal airways and acini over short-time intervals. We observed alternating patterns of R/D occurring within the same time frame in adjacent airspaces subtended by the same terminal airway. Using a computational model, we were able to simulate such alternating R/D phenomena during PCV, also mimicking how these phenomena varied with PEEP. Our model suggests that R/D over short-time scales occurs as a result of complex interactions between the time dependence of opening and closing pressures and the mechanical interdependence between neighboring lung units.

ACKNOWLEDGMENTS

We thank Thierry Brochard, Paul Tafforeau, Christian Nemoz, and Herwig Requardt (European Synchrotron Radiation Facility [ESRF]) for technical assistance, Hélène Bernard, Charlène Caloud, and Géraldine LeDuc for valuable help with the animal care. We thank Mats Wallin and Magnus Hallbäck (Maquet SA, Solna, Sweden) for their technical assistance with the mechanical ventilator. We are grateful to Emmanuel Brun (ESRF) for his help with the model algorithm.

REFERENCES

1. Dreyfuss D, Soler P, Basset G, et al: High inflation pressure pulmonary edema. Respective effects of high airway pressure, high tidal volume, and positive end-expiratory pressure. *Am Rev Respir Dis* 1988; 137:1159–1164
2. Muscedere JG, Mullen JB, Gan K, et al: Tidal ventilation at low airway pressures can augment lung injury. *Am J Respir Crit Care Med* 1994; 149:1327–1334
3. Slutsky AS, Ranieri VM: Ventilator-induced lung injury. *N Engl J Med* 2013; 369:2126–2136
4. dos Santos CC, Slutsky AS: Mechanotransduction, ventilator-induced lung injury and multiple organ dysfunction syndrome. *Intensive Care Med* 2000; 26:638–642
5. Taniguchi LU, Caldini EG, Velasco IT, et al: Cytoskeleton and mechanotransduction in the pathophysiology of ventilator-induced lung injury. *J Bras Pneumol* 2010; 36:363–371
6. Ventilation with lower tidal volumes as compared with traditional tidal volumes for acute lung injury and the acute respiratory distress syndrome. *N Engl J Med* 2000; 342:1301–1308
7. Peck MD, Koppelman T: Low-tidal-volume ventilation as a strategy to reduce ventilator-associated injury in ALI and ARDS. *J Burn Care Res* 2009; 30:172–175
8. Terragni PP, Rosboch G, Tealdi A, et al: Tidal hyperinflation during low tidal volume ventilation in acute respiratory distress syndrome. *Am J Respir Crit Care Med* 2007; 175:160–166
9. Slutsky AS: Lung injury caused by mechanical ventilation. *Chest* 1999; 116 (1 Suppl):9S–15S
10. Bachofen H, Schürch S, Michel RP, et al: Experimental hydrostatic pulmonary edema in rabbit lungs. Morphology. *Am Rev Respir Dis* 1993; 147:989–996

11. Hubmayr RD: Perspective on lung injury and recruitment: A skeptical look at the opening and collapse story. *Am J Respir Crit Care Med* 2002; 165:1647–1653
12. Mead J, Takishima T, Leith D: Stress distribution in lungs: A model of pulmonary elasticity. *J Appl Physiol* 1970; 28:596–608
13. Makiyama AM, Gibson LJ, Harris RS, et al: Stress concentration around an atelectatic region: A finite element model. *Respir Physiol Neurobiol* 2014; 201:101–110
14. Denny E, Schroter RC: A model of non-uniform lung parenchyma distortion. *J Biomech* 2006; 39:652–663
15. Bates JH, Irvin CG: Time dependence of recruitment and derecruitment in the lung: a theoretical model. *J Appl Physiol (1985)* 2002; 93:705–713
16. Bellardine CL, Hoffman AM, Tsai L, et al: Comparison of variable and conventional ventilation in a sheep saline lavage lung injury model. *Crit Care Med* 2006; 34:439–445
17. Ma B, Bates JH: Modeling the complex dynamics of derecruitment in the lung. *Ann Biomed Eng* 2010; 38:3466–3477
18. Smith BJ, Grant KA, Bates JH: Linking the development of ventilator-induced injury to mechanical function in the lung. *Ann Biomed Eng* 2013; 41:527–536
19. Smith BJ, Bates JH: Assessing the progression of ventilator-induced lung injury in mice. *IEEE Trans Biomed Eng* 2013; 60:3449–3457
20. Wilkins S, Gureyev T, Gao D, et al: Phase-contrast imaging using polychromatic hard X-rays. *Nature* 1996; 384:335–338
21. Bliznakova K, Russo P, Mettivier G, et al: A software platform for phase contrast x-ray breast imaging research. *Comput Biol Med* 2015; 61:62–74
22. Heil M, Hazel AL, Smith JA: The mechanics of airway closure. *Respir Physiol Neurobiol* 2008; 163:214–221
23. Kamm RD, Johnson M: Airway closure at low lung volume: The role of liquid film instabilities. *Appl Mech Rev* 1990; 43:S92–S97
24. Macklem PT, Proctor DF, Hogg JC: The stability of peripheral airways. *Respir Physiol* 1970; 8:191–203
25. Adler A, Bates JH: A micromechanical model of airway-parenchymal interdependence. *Ann Biomed Eng* 2000; 28:309–317
26. Smith BJ, Lundblad LKA, Kollisch-Singule M, et al: Predicting the response of the injured lung to the mechanical breath profile. *J Appl Physiol (1985)* 2015; 118:932–940
27. Hantos Z, Tolnai J, Asztalos T, et al: Acoustic evidence of airway opening during recruitment in excised dog lungs. *J Appl Physiol (1985)* 2004; 97:592–598
28. Victorino JA, Borges JB, Okamoto VN, et al: Imbalances in regional lung ventilation: A validation study on electrical impedance tomography. *Am J Respir Crit Care Med* 2004; 169:791–800